AD-A134 682 COMPARISON OF EXPERIMENTAL AND PREDICTED COLLAPSE PRESSURES FOR STIFFENED CYLINDRICAL SHELLS(U) NAVAL SURFACE WEAPONS CENTER SILVER SPRING MD M MOUSSOUROS

1/1

UNCLASSIFIED 01 SEP 82 NSWC/TR-83-20 F/G 12/1 NL

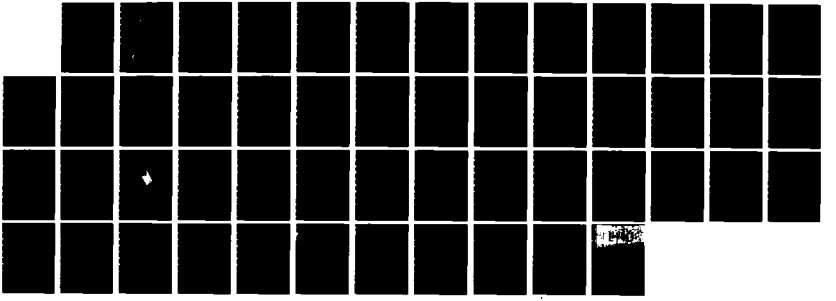

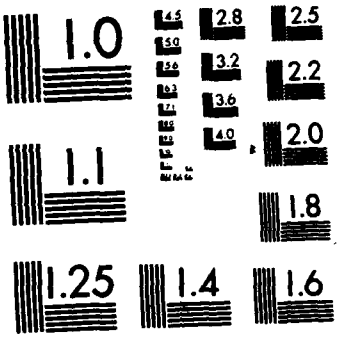

MICROCOPY RESOLUTION TEST CHART
NATIONAL BUREAU OF STANDARDS-1963-A

(12)

NSWC TR 33-20

AD-A134 682

COMPARISON OF EXPERIMENTAL AND PREDICTED COLLAPSE PRESSURES FOR STIFFENED CYLINDRICAL SHELLS

BY DR. MINOS MOUSSOURIS

RESEARCH AND TECHNOLOGY DEPARTMENT

1 SEPTEMBER 1982

Approved for public release, distribution unlimited.

DTIC FILE COPY

ELECTE
NOV 1 0 1983
A

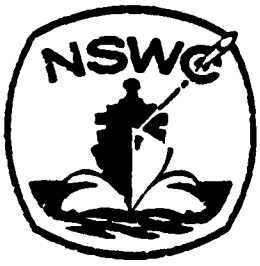

NAVAL SURFACE WEAPONS CENTER

Dahlgren, Virginia 22448 • Silver Spring, Maryland 20910

83 11 10 034

UNCLASSIFIED

SECURITY CLASSIFICATION OF THIS PAGE (When Data Entered)

REPORT DOCUMENTATION PAGE

READ INSTRUCTIONS BEFORE COMPLETING FORM

1. REPORT NUMBER	2. GOVT ACCESSION NO.	3. RECIPIENT'S CATALOG NUMBER
NSWC TR 83-20		

4. TITLE (and Subtitle)	5. TYPE OF REPORT & PERIOD COVERED
COMPARISON OF EXPERIMENTAL AND PREDICTED COLLAPSE PRESSURES FOR STIFFENED CYLINDRICAL SHELLS	Documentation
	6. PERFORMING ORG. REPORT NUMBER

7. AUTHOR(s)	8. CONTRACT OR GRANT NUMBER(s)
Dr. Minos Moussouros	

9. PERFORMING ORGANIZATION NAME AND ADDRESS	10. PROGRAM ELEMENT, PROJECT, TASK AREA & WORK UNIT NUMBERS
Naval Surface Weapons Center (Code R14) White Oak Silver Spring, MD 20910	63610N; 50-199-600-0-2R19BB429

11. CONTROLLING OFFICE NAME AND ADDRESS	12. REPORT DATE
	1 September 1982
	13. NUMBER OF PAGES
	47

14. MONITORING AGENCY NAME & ADDRESS(if different from Controlling Office)	15. SECURITY CLASS. (of this report)
	UNCLASSIFIED
	15a. DECLASSIFICATION/DOWNGRADING SCHEDULE

16. DISTRIBUTION STATEMENT (of this Report)

Approved for public release; distribution unlimited.

17. DISTRIBUTION STATEMENT (of the abstract entered in Block 20, if different from Report)

18. SUPPLEMENTARY NOTES

19. KEY WORDS (Continue on reverse side if necessary and identify by block number)

Static Collapse
Buckling
Structural Instability
Shells
Stiffened Shells

20. ABSTRACT (Continue on reverse side if necessary and identify by block number)

The finite element code STAGS is used to obtain buckling load predictions for a number of ring reinforced circular cylindrical shells for which experimental results are reported in the open literature. However, as the thickness of pressure hulls increases and the ratio of radius to thickness decreases, failure may occur by plastic yielding and axisymmetric collapse at a limit point. For these cases, predictions using STAGS are substantially less successful. The possible existence of locked-in residual stresses or strains

DD FORM 1 JAN 73 1473 EDITION OF 1 NOV 68 IS OBSOLETE
S/N 0102-LF-014-6601

UNCLASSIFIED
SECURITY CLASSIFICATION OF THIS PAGE (When Data Entered)

20. (Cont.)

is another source of discrepancy. Agreement is reasonable, especially in the elastic range, in view of the difficulties of this type of analysis.

FOREWORD

The finite element code STAGS is used to obtain buckling load predictions for a number of ring reinforced circular cylindrical shells for which experimental results are reported in the open literature. However, as the thickness of pressure hulls increases and the ratio of radius to thickness decreases, failure may occur by plastic yielding and axisymmetric collapse at a limit point. For these cases, predictions using STAGS are substantially less successful. The possible existence of locked-in residual stresses or strains is another source of discrepancy. Agreement is reasonable, especially in the elastic range, in view of the difficulties of this type of analysis.

This work represents three work-months of effort under funding of the Naval Sea Systems Command, whose support is gratefully acknowledged.

Approved by:

J. F. PROCTOR, Head
Energetic Materials Division

DTIC COPY INSPECTED

A-1

CONTENTS

Chapter		Page
1	INTRODUCTION	1
2	ANALYSIS	2
3	DISCUSSION OF RESULTS	5
4	SUMMARY	9

ILLUSTRATIONS

Figure		Page
1	FULL CYLINDER CIRCUMFERENTIALLY AND HALF AXIALLY DISPLAYING CIRCULAR ENDS 4 AND 3 AND ASSUMED LONGITUDINAL ENDS 2 AND 4 AT $\theta=0$ and $\theta=\pi$ RESPECTIVELY	10
2	MODE 1 FOR MODEL 1, HALF MODEL OF BR-5	11
3	MODE 1 FOR MODEL 2, FULL MODEL OF BR-5	12
4	MODE 1 FOR MODEL 1A (BR-5 INCLUDING 1 BAY WITH BULKHEAD) SUBJECT TO CONTINUITY CONDITIONS AND W=0 AT BULKHEAD END.	13
5	EXTERNAL PRESSURE-DEFLECTION/THICKNESS CURVE OF MODEL 3 UP TO APPROXIMATE STATIC COLLAPSE	14
6	MODE 1 FOR MODEL 4 (ALUMINUM MODEL G OF MIDGLEY AND JOHNSON) SUBJECT TO SIMPLY SUPPORTED CONDITIONS AT END 1	15
7	MODE 1 FOR MODEL 5 (ALUMINUM MODEL G OF MIDGLEY AND JOHNSON) SUBJECT TO CONTINUITY END CONDITIONS AND W≠0 AT END 1	16
8	MODE 1 FOR MODEL 6 (ALUMINUM MODEL G OF MIDGLEY AND JOHNSON) SUBJECT TO CONTINUITY CONDITIONS AND W=0 AT END 1	17
9	MODE 1 FOR MODEL 8 (ALUMINUM MODEL F OF MIDGLEY AND JOHNSON) SUBJECT TO SIMPLY SUPPORTED CONDITIONS AT END 1	18
10	MODE 1 FOR MODEL 9 (ALUMINUM MODEL F OF MIDGLEY AND JOHNSON) SUBJECT TO CONTINUITY CONDITIONS AND W≠0 WITHOUT END RING AT END 1	19
11	MODE 1 FOR MODEL 10 (ALUMINUM MODEL F OF MIDGLEY AND JOHNSON) SUBJECT TO CONTINUITY CONDITIONS AND W≠0, WITH END RING AT END 1	20
12	MODE 1 FOR MODEL 11 (ALUMINUM MODEL F OF MIDGLEY AND JOHNSON) SUBJECT TO CONTINUITY CONDITIONS AND W=0 AT END 1	21
13	MODE 1 FOR MODEL 12 (STEEL 1/5 SCALE MODEL OF KINRA) SUBJECT TO CONTINUITY CONDITIONS AND W=0 AT END 1	22

ILLUSTRATIONS (Cont.)

Figure		Page
14	MODE 1 FOR MODEL 13 (BR-4, EXTERNALLY STIFFENED STEEL MODEL) SUBJECT TO CONTINUITY CONDITIONS AND W=0 AT END 1	23
15	DEFORMED SHAPE OF MODEL 14 (STEEL MODEL BR-4) AT 500 LB/IN^2 .	24
16	MODE 1 FOR MODEL 17 (1.965 LONGER THAN MODEL 8) SUBJECT TO SIMPLY SUPPORTED CONDITIONS AT END 1	25
17	MODE 1 FOR MODEL 18 (1.965 LONGER THAN MODEL 9) SUBJECT TO CONTINUITY CONDITIONS AND W≠0, WITHOUT END RING AT END 1	26
18	MODE 1 FOR MODEL 19 (1.965 LONGER THAN MODEL 10) SUBJECT TO CONTINUITY CONDITIONS AND W≠0, WITH END RING AT END 1 . . .	27
19	MODE 1 FOR MODEL 20 (1.965 LONGER THAN MODEL 11) SUBJECT TO CONTINUITY CONDITIONS AND W=0 AT END 1	28

TABLES

Table		Page
1	TEST MODEL STRUCTURAL DETAILS	29
2	TEST MODEL MATERIAL DETAILS	31
3	ACTUAL DIMENSIONS USED IN COMPUTATIONS	32
4	MODELING DETAILS	33
5	COMPARISON BETWEEN FINITE ELEMENT ANALYSIS PREDICTIONS AND EXPERIMENTAL RESULTS	36

CHAPTER 1

INTRODUCTION

The ultimate objective of this work is to establish reliable finite element procedures for predicting the effect of structural damage, for example due to a shock wave, on the collapse strength of submarine hulls. However, it is first necessary to demonstrate the validity of finite element calculations for undamaged structures. Unfortunately, the open literature provides little information on finite element code validation for buckling of stiffened structures.

In two previous studies by the current author,[1,2] predictions using the code STAGS[3] were compared to those from other methods in the open literature. The present report compares STAGS predictions to published experimental results from seven different tests. The agreement is reasonable, particularly in view of the difficulties of this type of analysis.

[1]Moussouros, M., Comparisons of Static Collapse Pressure Predictions of a Ring-Stiffened Cylindrical Shell Subject to Hydrostatic Pressure, NSWC TR 81-325, 3 Mar 1982.

[2]Moussouros, M., Further Results on the Predictions of Collapse Pressure of a Ring-Stiffened Cylindrical Shell Subject to Hydrostatic Pressure, NSWC TR 82-172, Sep 1982.

[3]Almroth, B. O., Brogan, F. A., and Stanley, G. M., Structural Analysis of General Shells, Vol. II, User Instruction for STAGSC, LMSC-D633873, Apr 1979.

CHAPTER 2

ANALYSIS

A number of papers in the open literature contain experimental collapse pressure values for ring-stiffened cylindrical shells.[4-16]

[4]Slankard, R. C., and Nash, W. A., Tests of the Elastic Stability of a Ring-Stiffened Cylindrical Shell, Model BR-5 (λ=1.705, Subjected to Hydrostatic Pressure, DTMB Report 822, May 1953.

[5]Slankard, R. C., Tests of Elastic Stability of a Ring-Stiffened Cylindrical Shell, Model BR-4 (λ=1.103) Subjected to Hydrostatic Pressure, DTMB Report 876, Feb 1955.

[6]Kirstein, A. F., and Slankard, R. C., An Experimental Investigation of the Shell-Instability Strength of a Machined, Ring-Stiffened Cylindrical Shell Under Hydrostatic Pressure (Model BR-4A), DTMB Report 997, Apr 1956.

[7]Lunchick, M., and Overby, J. A., An Experimental Investigation of the Yield Strength of a Machined Ring-Stiffened Cylindrical Shell (Model BR-7M) Under Hydrostatic Pressure, DTMB Report 1255, Nov 1958.

[8]DeHart, R., and Basdekas, N. L., "Investigation of Yield Collapse of Stiffened Circular Cylindrical Shells with a Given Out-of-Roundness," in Collected Papers on Instability of Shell Structures-1962, NASA TN D-1510, 1962, pp. 245-253.

[9]Midgley, W. R., and Johnson, A. E., Jr., "Experimental Buckling of Internal Integral Ring-Stiffened Cylinders," Experimental Mechanics, Jul 1973, pp. 145-153.

[10]Kinra, R. K., "Hydrostatic and Axial Collapse Tests of Stiffened Cylinders," Paper 2685 in Offshore Technology Conference, 1976, pp. 765-788.

[11]Galletly, G. D., Slankard, R. C., and Wenk, E., Jr., "General Instability of Ring-Stiffened Cylindrical Shells Subject to External Hydrostatic Pressure--A Comparison of Theory," Journal of Applied Mechanics, Vol. 25, No. 2, Jun 1958, pp. 259-266.

[12]Reynolds, T. E., and Blumenberg, W. F., General Instability of Ring-Stiffened Shells Subject to External Hydrostatic Pressure, DTMB Report 1324, Jun 1959.

Several of these studies[17-23] provide enough data to permit modeling (e.g., model design, material properties). Unfortunately, in our judgment, the remainder[24-29] do not give sufficient information, but they are listed here for completeness.

Table 1 gives the structural details of the models to be examined, while Table 2 gives material properties.

The various models have been analyzed using the general purpose finite element code STAGS. Tables 3 and 4 show details of the finite element analysis, including the dimensions actually used in the computations, the number of

[13]Krenzke, M. A., Effect of Initial Deflections and Residual Welding Stresses of Elastic Behavior and Collapse Pressure of Stiffened Cylinders Subjected to External Hydrostatic Pressure, DTMB Report 1327, Apr 1960.

[14]Blumenberg, W. F., and Reynolds, T. E., Elastic Instability of Ring-Stiffened Cylinders with Intermediate Heavy Frames Under External Hydrostatic Pressure, DTMB Report 1588, Dec 1961.

[15]Blumenberg, W. F., Hydrostatic Pressure Tests to Determine the Effect of Varying Degrees of End Fixity on the Elastic General Instability Strength of Ring-Stiffened Cylindrical Shells, DTMB Report 2361, May 1967.

[16]Batista, R. C., and Croll, J. G. A., "Simple Buckling for Pressurized Cylinders," Journal of Engineering Mechanics EM5, ASCE, Oct 1982, pp.927-944.

[17]Slankard, DTMB Report 822.

[18]Slankard, DTMB Report 876.

[19]Kirstein, DTMB Report 997.

[20]Lunchick, DTMB Report 1255.

[21]DeHart, NASA TN D-1510.

[22]Midgley, pp. 145-153.

[23]Kinra, pp. 765-788.

[24]Galletly, pp. 259-266.

[25]Reynolds, DTMB Report 1324.

[26]Krenzke, DTMB Report 1327.

[27]Blumenberg, DTMB Report 1588.

[28]Blumenberg, DTMB Report 2361.

[29]Bastista, pp. 927-944.

degrees of freedom (D.O.F.), the distribution of nodes, and the boundary conditions. The models are assumed to be perfectly circular. They are discretized using flat plate quadrilateral elements, specifically the STAGS 410 element. Rigid body modes are removed with appropriate constraints. Axial loads are imposed as equivalent line loads along the end plate perimeters. This method neglects local bending at end plate intersections. Finally the "dead pressure" is used. The base load pressure used in 1 lb/in^2 and the linear option (linear stress state) of STAGS is exercised, unless otherwise mentioned. Figure 1 illustrates the coordinate system and the notation to be used to denote the displacements.

CHAPTER 3

DISCUSSION OF RESULTS

Table 5 displays the numerical results obtained using STAGS, i.e., critical pressures for static collapse, buckling mode, type of boundary conditions used in the analysis, and type of stiffening. Also shown are experimental collapse values and collapse modes where available.

Note that Models 1 and 2 give a buckling pressure of 106.3 lb/in^2 for Model 1 and 102.6 lb/in^2 for Model 2 with correspnding oval modes (Figures 2 and 3), indicating stiffener collapse.* Also note that the half and full models circumferentially do not give identical critical pressures, although both computations are carried out using the same base load. Model 1A, which incorporates an additional shorter frame spacing with a rigid bulkhead, results in a higher critical pressure of 155.596 lb/in^2 and a lobar mode of collapse (Figure 4). For Model 1A, the maximum axial and hoop stresses are -28.785 ksi and -35.631 ksi, respectively. The lower experimental pressure (80 lb/in^2) is attributed to residual strains (model was not stress relieved) rather than to imperfections, considering that in the case of ring-stiffened cylinders, the rings in a sense constitute imperfections far larger in magnitude than the ones due to fabrication. There is an undeniable influence due to imperfections, however, which according to Coppa[30] is smoothed out with increasing pressure, except for these imperfections due to the rings themselves. The case of axial compression only is excluded in this discussion.

A nonlinear incremental analysis was performed for Model 3 (Figure 5). It was discontinued at a pressure 9500 lb/in^2 due to a large step size increment. This is comparable to the experimental collapse pressure of 9750 lbs/in^2. Note that the slope of the pressure-displacement curve on Figure 5 is decreasing rapidly in this vicinity.

Model 4 (simply supported at end 1) buckled in a lobar pattern (Figure 6) at 23.704 lb/in^2, while Model 5 (Figure 7) with continuity conditions at end 1 ovalized at 21.262 lb/in^2. Model 6 with W = 0 at end 1 (effect of bulkhead) buckled at 23.669 lb/in^2 in a diamond shape mode between rings (Figure 8).

*In Figure 2, the stiffener at midlength is shown displaced radially inwards.

[30] Coppa, A. P., "Measurement of Initial Geometrical Imperfections of Cylindrical Shells," AIAA Journal, Vol. 4, No. 1, Jan 1966, pp. 172-175.

According to Midgley and Johnson,[31] the stiffeners were overdesigned to localize the instability between successive rings. Model 7 was treated using an incremental nonlinear analysis. When discontinued at 31 lb/in^2, the model had not attained the collapse pressure. The experimental collapse pattern given is that of Midgley and Johnson.[32] Overall, if we are to take the first value given (25 lb/in^2), the finite element program STAGS gives a fairly good estimate for this model. The experimental model represented by Models 4 through 7 was a machined structure.

Models 9 and 10 (Figures 10 and 11) yield collapse pressures well below the lowest experimental value (65 in/in^2) reported. Models 8 and 11 (Figures 9 and 12) failed by overall instability at 62.651 lb/in^2 and 62.371 lb/in^2, respectively. These models were based on Model F.[33] The ring stiffeners were underdesigned, unable to prevent overall collapse or restrict buckling between them. Figures 9 through 12 exhibited overall instability, confirmed by Midgley and Johnson.[34] An oval critical mode was obtained when continuity conditions at end 1, without an end ring (Model 9 of Figure 10), were used and also when an end ring was employed (Model 10 of Figure 11). Since the stiffeners were not strong enough, they collapsed according to the ring formula,[35] which in this case gives 5.266 lb/in^2 (Table 5). The experimental model represented by Models 8 through 11 was a machined structure.

On the other hand, Southwell's formula,[36] treating the shell as fully unstiffened, yields about 6.60 in/in^2 (this is not included in Table 5) as the collapse pressure. Using Brush and Almroth's Figure 5.17 or 5.11[37] with L = 18.85 in., a = 7.955 in., h = 0.040 in., $\underline{E}$ = 10.10 x 10^6 lb/in^2, ν = 0.300, D = 59.194 lb-in., Z = 1065.8, we obtain $\underline{p} \sim 36$ and, therefore, the critical collapse pressure is 7.43 lb/in^2. It is evident from this analysis that only a very long cylinder with weak stiffeners should buckle as displayed on Figures 10 and 11. On the other hand, when the stiffeners are strong (Figure 7 of Model 5), we may still obtain a relatively accurate estimate of the critical pressure. It is, however, associated with the wrong mode. At first sight, it appears that the computed collapse pressures for Models 2 and 4 are reasonably good, although the predicted collapse modes are not. It is considered that their apparent good agreement should not be trusted too much. As discussed in the next paragraph, the lower experimental pressure is probably due to residual strains and initial imperfections in this welded cylindrical model.

---

[31]Midgley, pp. 145-153.

[32]Midgley, pp. 145-153.

[33]Midgley, pp. 145-153.

[34]Midgley, pp. 145-153.

[35]Moussouros, NSWC TR 82-172.

[36]Moussouros, NSWC TR 81-325.

[37]Brush, D. O., and Almroth, B. O., Buckling of Bars, Plates, and Shells, McGraw Hill, Inc., 1975, pp. 161-167.

Model 12 (Figure 13) clearly shows lobar buckling between rings at a higher pressure (161.19 lb/in^2) reported on Table 5 (110-115 lb/in^2). Another unreported model, with frame spacing twice that of Model 12, collapsed at 78.668 lb/in^2 in the lobar mode. The experimental model represented by Model 12 was a welded structure.

Model 13 (Figure 14) collapsed at 536.058 lb/in^2 in a lobar mode. At this pressure, a hoop stress of -58.96 ksi (higher than yield) developed and the linear stress state must be abandoned. Model 14 (Figure 15), which exhibited plastic deformation, had not failed up to a pressure of 512.5 lb/in^2. At this point, it appears that residual stresses were the cause of this large discrepancy (390 in/in^2). A model identical to BR-4, but stress relieved, failed at 550 lb/in^2 (compared to 390 in/in^2, which includes residual stresses).[38] This is close to the reported collapse pressure by Bushnell[39] and the BASOR program (460 lb/in^2).

In Model 15, collapse pressure predictions ignoring plasticity are much higher than the experimental values used and should be disregarded. Model 16 is treated by nonlinear analysis; it did not collapse up to 1500 lb/in^2. It must be stressed at this point that except for Model 3, for which the stress strain curve was given, the stress strain curve had to be approximated and adjusted, causing another source of differences.

Models 17, 18, 19, and 20 (Figures 16, 17, 18 and 19) collapsed in a fashion similar to Models 8, 9, 10, and 11 respectively, but at lower critical pressures, since their length was larger. Observe that the critical collapse pressures for Models 18 and 19 (4.13 lb/in^2 and 4.268 lb/in^2) using continuity conditions at end 1 were only about 50% of the critical pressure for Models 9 and 10 (7.257 lb/in^2 and 7.524 lb/in^2). This ratio (0.569 to 0.567) in critical pressure was not the same for Models 17 and 20 (19.893 lb/in^2 and 20.277 lb/in^2) as compared to Models 8 and 11 (62.651 lb/in^2 and 62.371 lb/in^2). This last range of ratios in critical pressure, as ℓ is reduced to 0.5089ℓ, becomes 0.317 to 0.325, suggesting a trend similar to a strut. These comments follow, since the mode here is that of general instability in the elastic range. It is known that, when the length of a strut is increased from ℓ_1 to ℓ_2, the critical pressure within the elastic range is reduced to the ratio $(\ell_1/\ell_2)^2$. In this case, the new critical pressures for Models 17 and 20 should have been 0.2589 of the critical pressures of Models 8 and 11 respectively, i.e., 16.22 lb/in^2 and 16.15 lb/in^2 (compare with 19.893 lb/in^2 and 20.277 lb/in^2 of Table 5).

A portion of Table 5 was compiled using various formulae in the open literature to give an estimate of the critical pressure at which buckling is to occur, in theory, at least in the elastic range. Furthermore, it provides estimates to the collapse of ring stiffeners subject to live pressure. Note that for Models 4 through 7 (Model G)[40], for which the stiffeners were not

---

[38]Kirstein, DTMB Report 997.

[39]Bushnell, D., "Effect of Cold Bending and Welding on Buckling of Ring-Stiffened Cylinders," Journal of Computers and Structures, Vol. 12, 1980, pp. 291-307.

[40]Midgley, pp. 145-153.

underdesigned, the critical pressure for ring buckling by Table 5 is 16.410 lb/in^2, while the experimental collapse of the shell 25 lb/in^2. The Southwell method[41] yielded 19.585 lb/in^2 and the Von Mises[42] 23.091 lb/in^2, respectively, for Models 4 through 7. The point to be conveyed is that when the approximate theoretical formulae define critical collapse pressures of the same relative magnitude as STAGS, with stresses below the yield point, buckling probably occurs between the stiffeners in a diamond-shape fashion. On the other hand, when approximate formulae suggest critical buckling pressures for a ring stiffener well below the finite element predicted value with stresses below yield, the probable mode of collapse would be overall instability, such as in Models 8 through 11 and 7 through 20 (Table 5).

[41]Moussouros, NSWC TR 81-325.

[42]Moussouros, NSWC TR 81-325.

CHAPTER 5

SUMMARY

This report compares finite element static pressure predictions to experimental values reported in the open literature. As expected, there are discrepancies between these values. The most obvious one appears to be residual stresses or strains.

Simply supported or clamped (as defined here) end conditions lead to similar predictions for the buckling pressures. Continuity conditions, in general, may give the buckling pressure for a ring (oval mode), but it may be preferable not to use them except when the stiffeners are especially heavy.[43]

Considering the overall performance of STAGS, it is safe to say that, with some exceptions, it has had some success in predicting critical pressures, especially in the elastic range. However, as the thickness of pressure hulls increases and R/h decreases, failure may occur by plastic yielding and axisymmetric collapse at a limit point. For these cases, predictions using STAGS are substantially less successful. It must be further stressed, however, that in all likelihood, even in the plastic range, the presence of the rings, viewed as an imperfection, will dominate buckling.

In closing it must be mentioned that it is hoped to overcome some of the limitations of the current analysis in the future by exploiting

(i) a different analysis option of STAGS

(ii) better experimental data

(iii) other computer codes such as BOSOR, ABAQUS or any other technique that may become available in the meantime.

[43] Moussouros, NSWC TR 81-325.

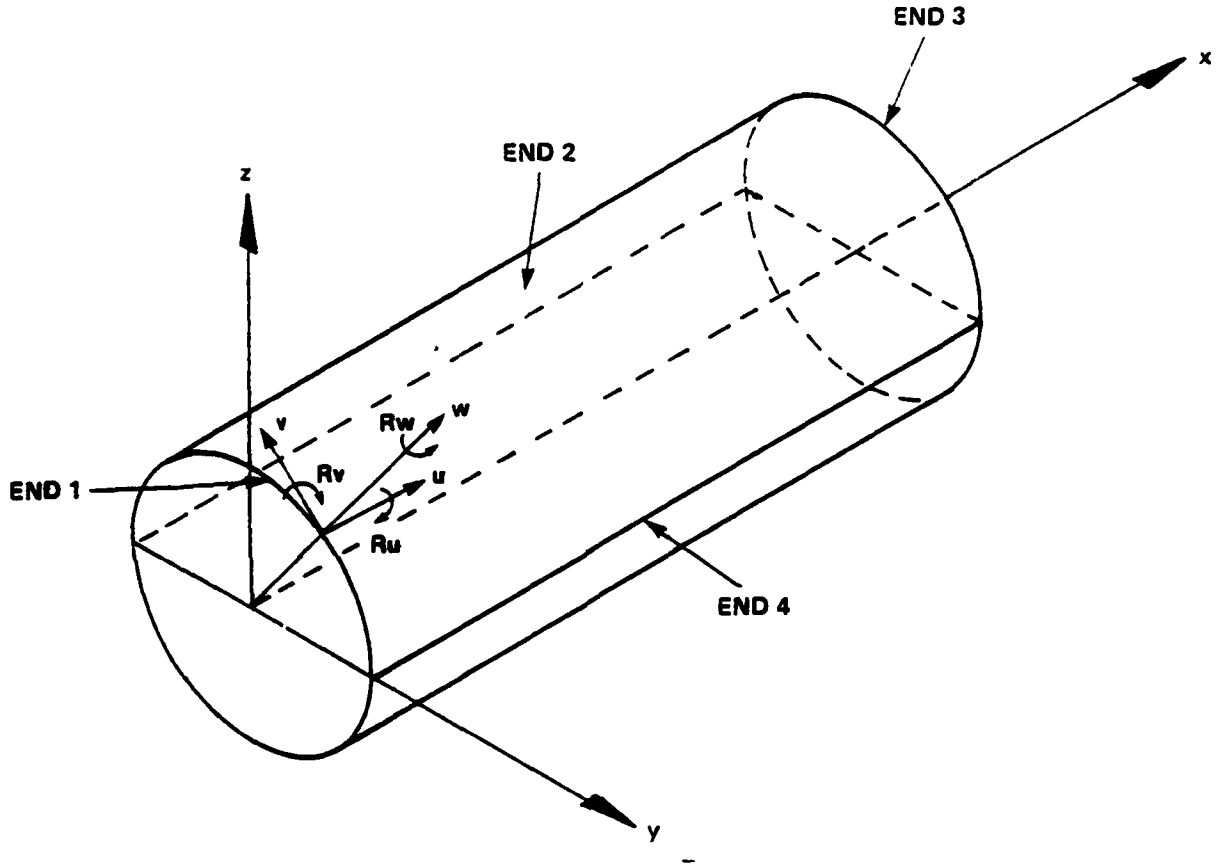

u = Axial displacement (along global longitudinal axis)
v = Tangential displacement (along local axis)
w = Radial displacement (along local radial axis)
Ru = Rotation about longitudinal axis x
Rv = Rotation about local tangential axis v
Rw = Rotation about local radial axis w

FIGURE 1. FULL CYLINDER CIRCUMFERENTIALLY AND HALF AXIALLY DISPLAYING CIRCULAR ENDS 4 AND 3 AND ASSUMED LONGITUDINAL ENDS 2 AND 4 AT $\theta = 0$ AND $\theta = \pi$ RESPECTIVELY

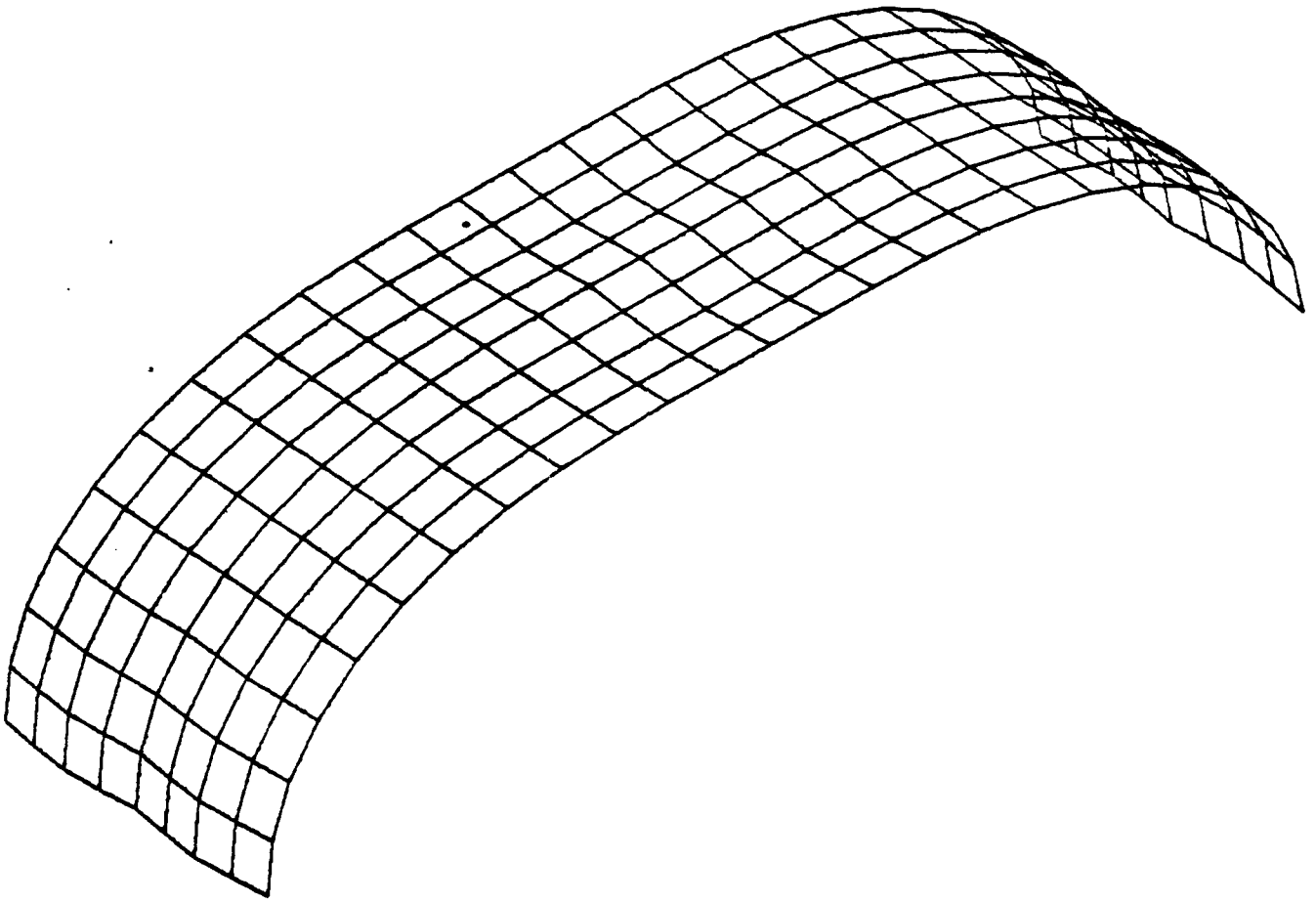

FIGURE 2. MODE 1 FOR MODEL 1, HALF MODEL OF BR-5

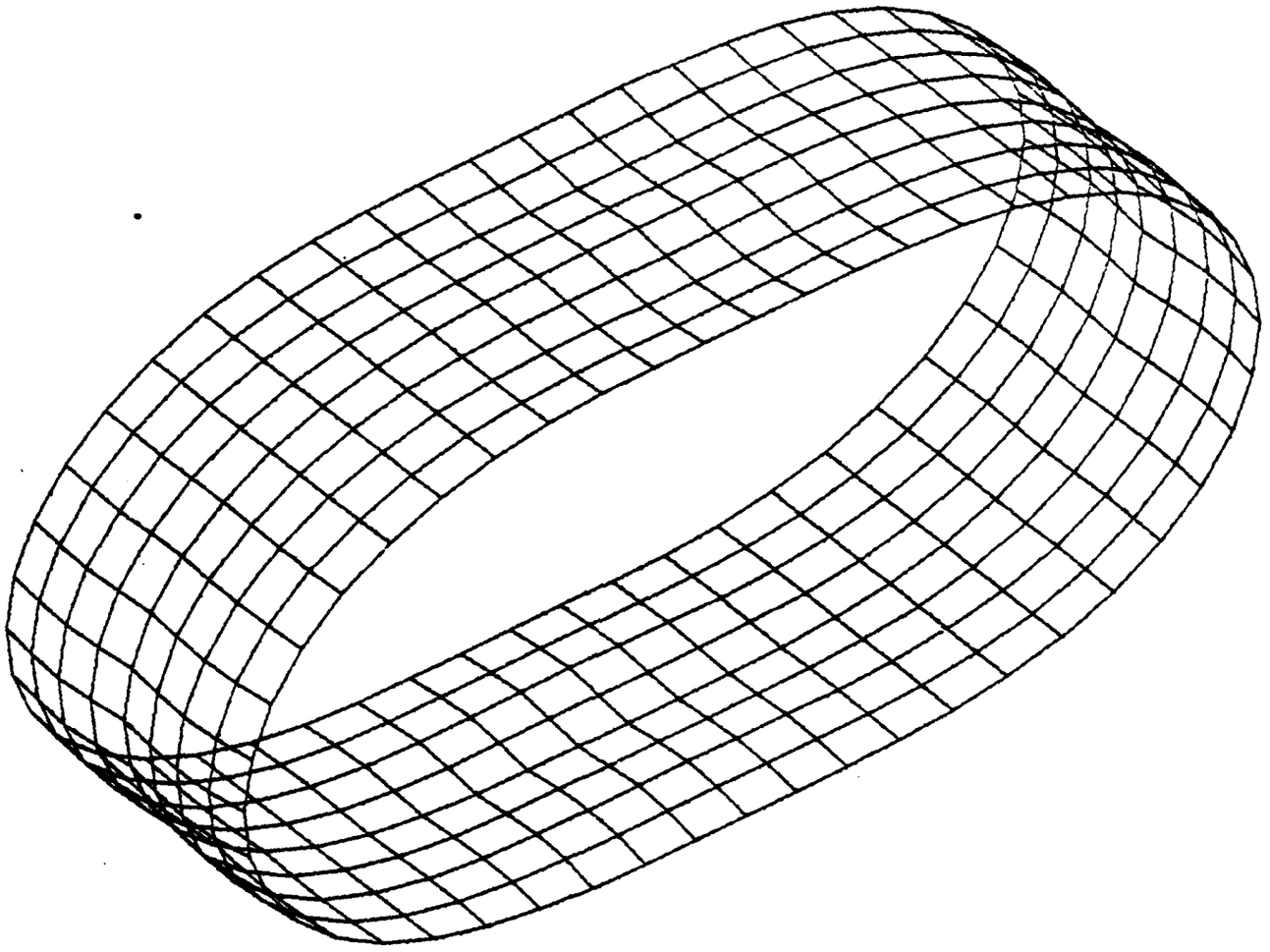

FIGURE 3. MODE 1 FOR MODEL 2, FULL MODEL OF BR-5

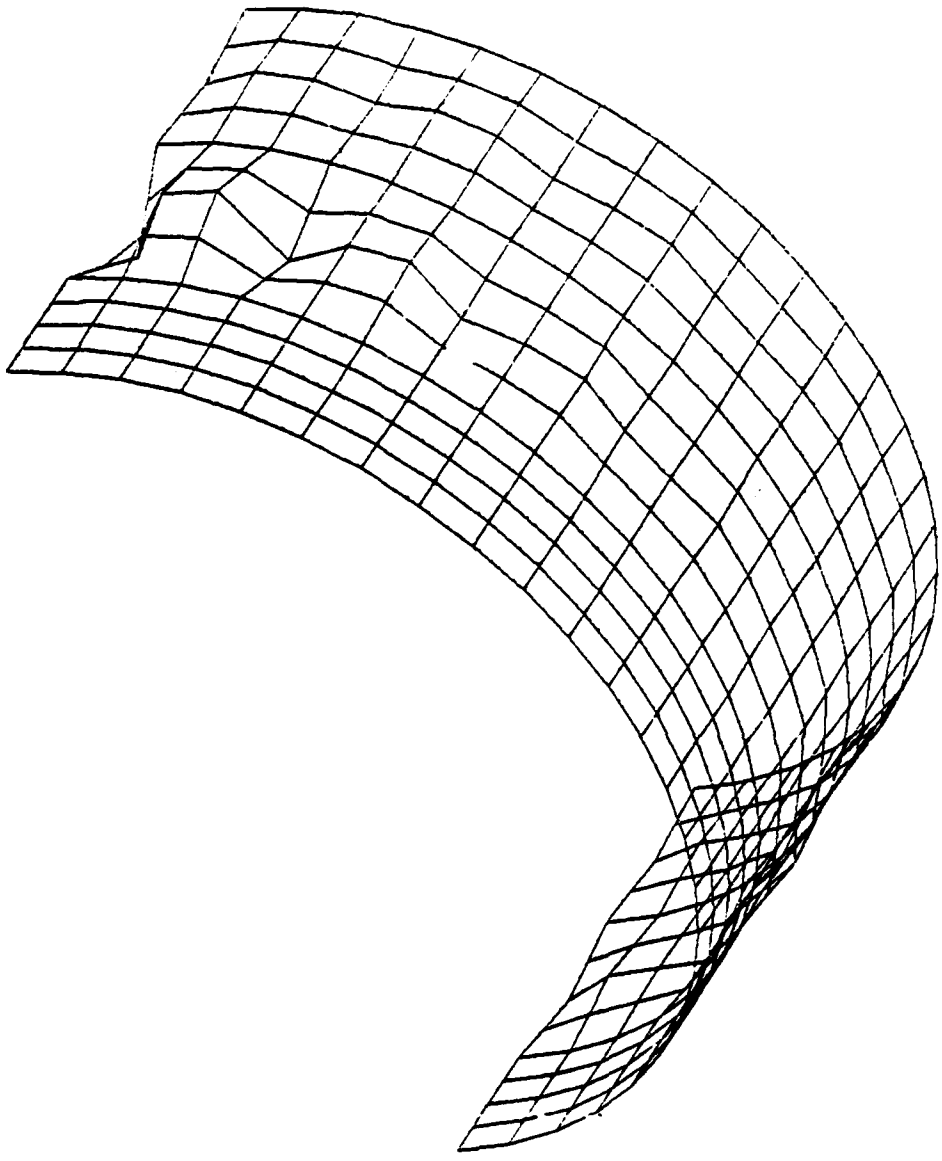

FIGURE 4. MODE 1 FOR MODEL 1A (BR-5 INCLUDING 1 BAY WITH BULKHEAD) SUBJECT TO CONTINUITY CONDITIONS AND W=0 AT BULKHEAD END

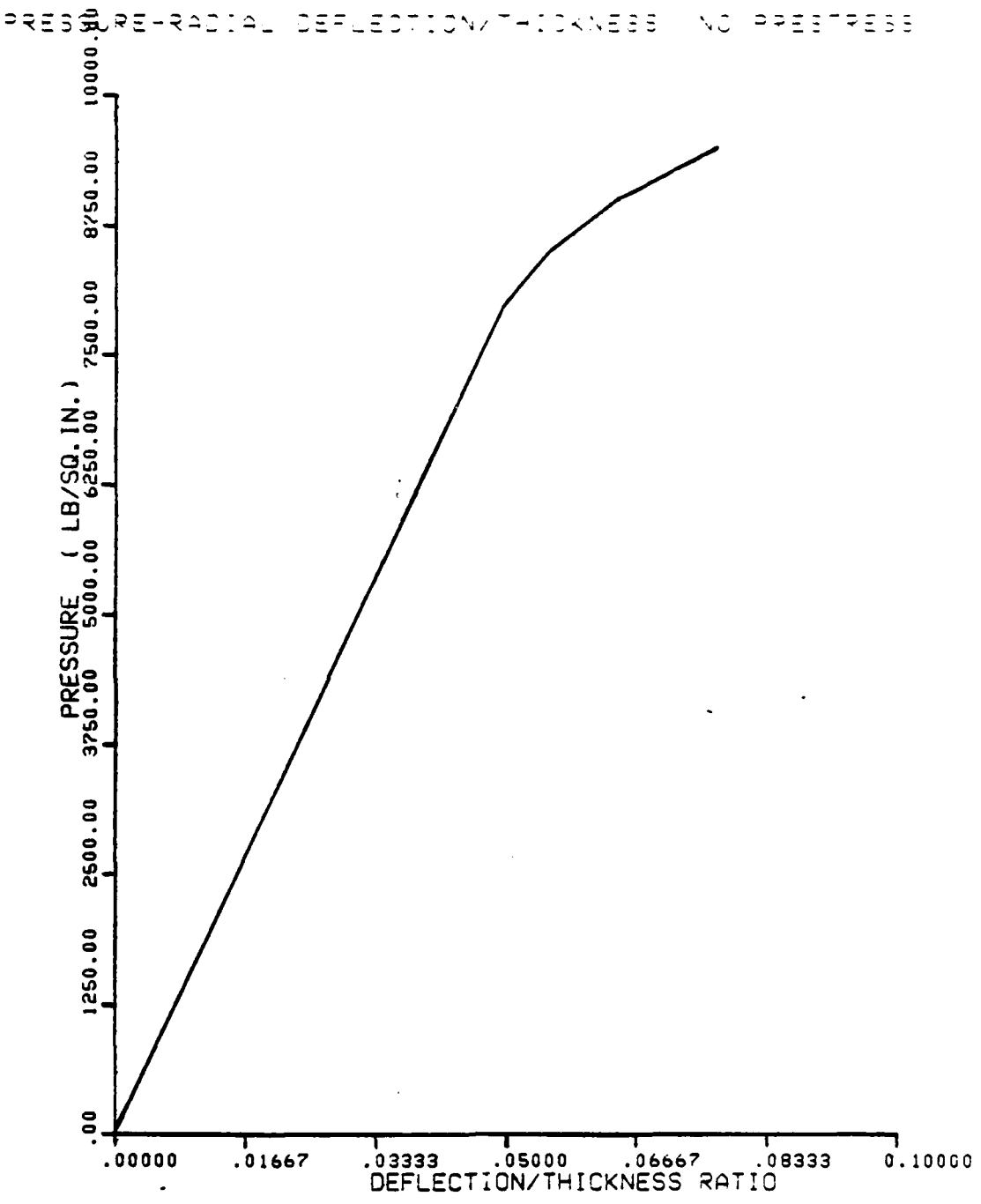

FIGURE 5. EXTERNAL PRESSURE DEFLECTION/THICKNESS CURVE OF MODEL 3 UP TO APPROXIMATE STATIC COLLAPSE

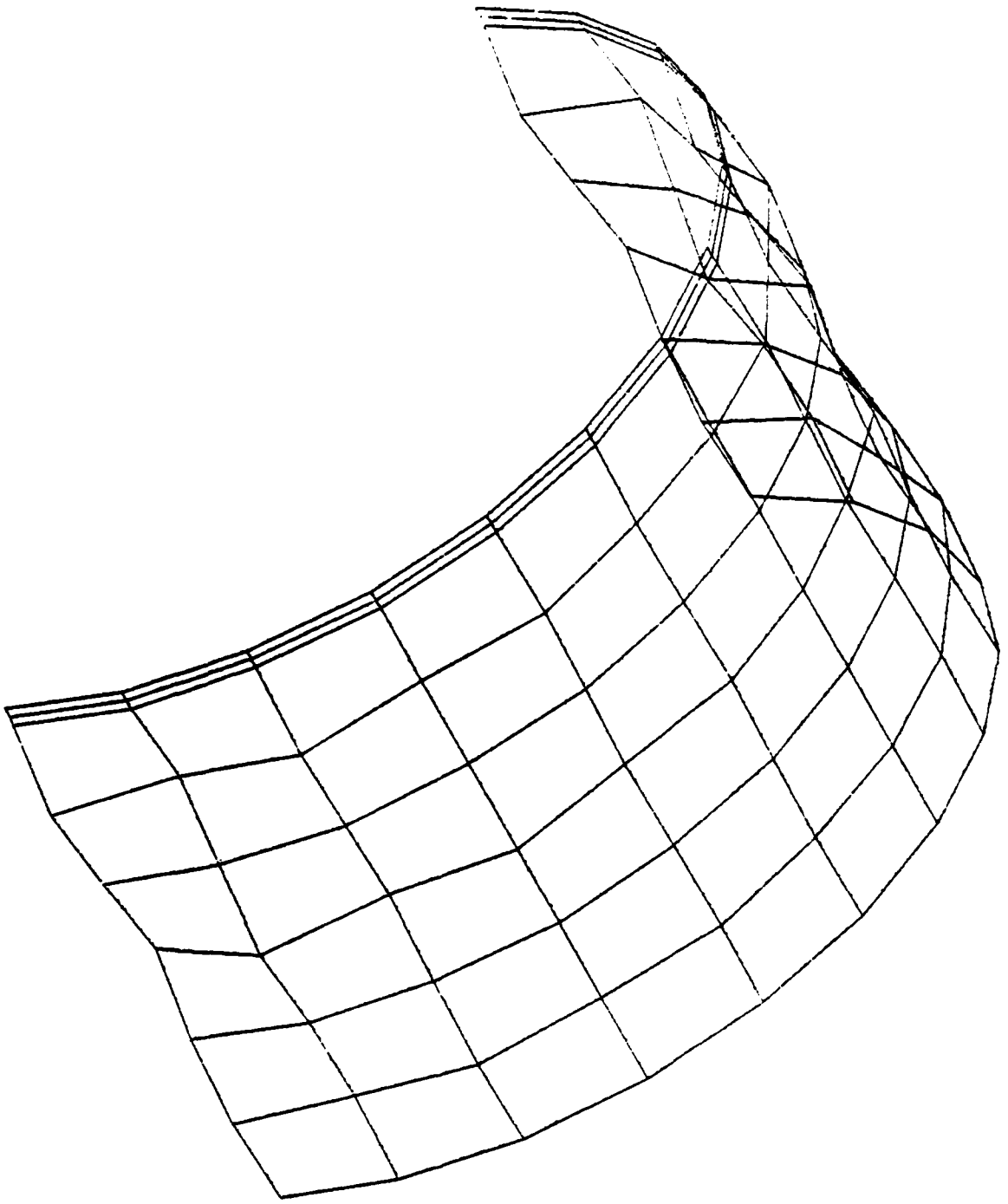

FIGURE 6. MODE 1 FOR MODEL 4 (ALUMINUM MODEL G OF MIDGLEY AND JOHNSON) SUBJECT TO SIMPLY SUPPORTED CONDITIONS AT END 1

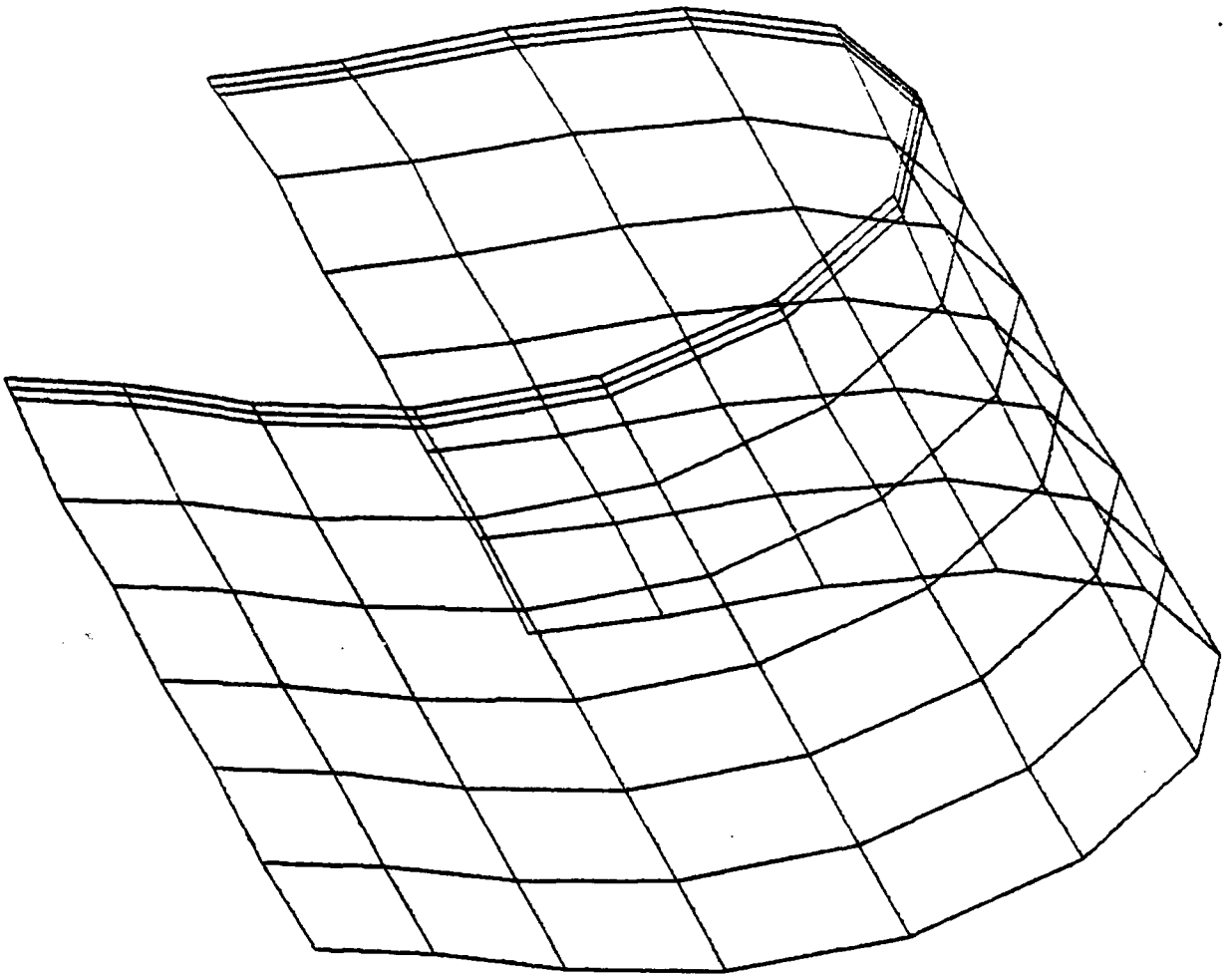

FIGURE 7. MODE 1 FOR MODEL 5 (ALUMINUM MODEL G OF MIDGLEY AND JOHNSON) SUBJECT TO CONTINUITY END CONDITIONS AND $W \neq 0$ AT END 1

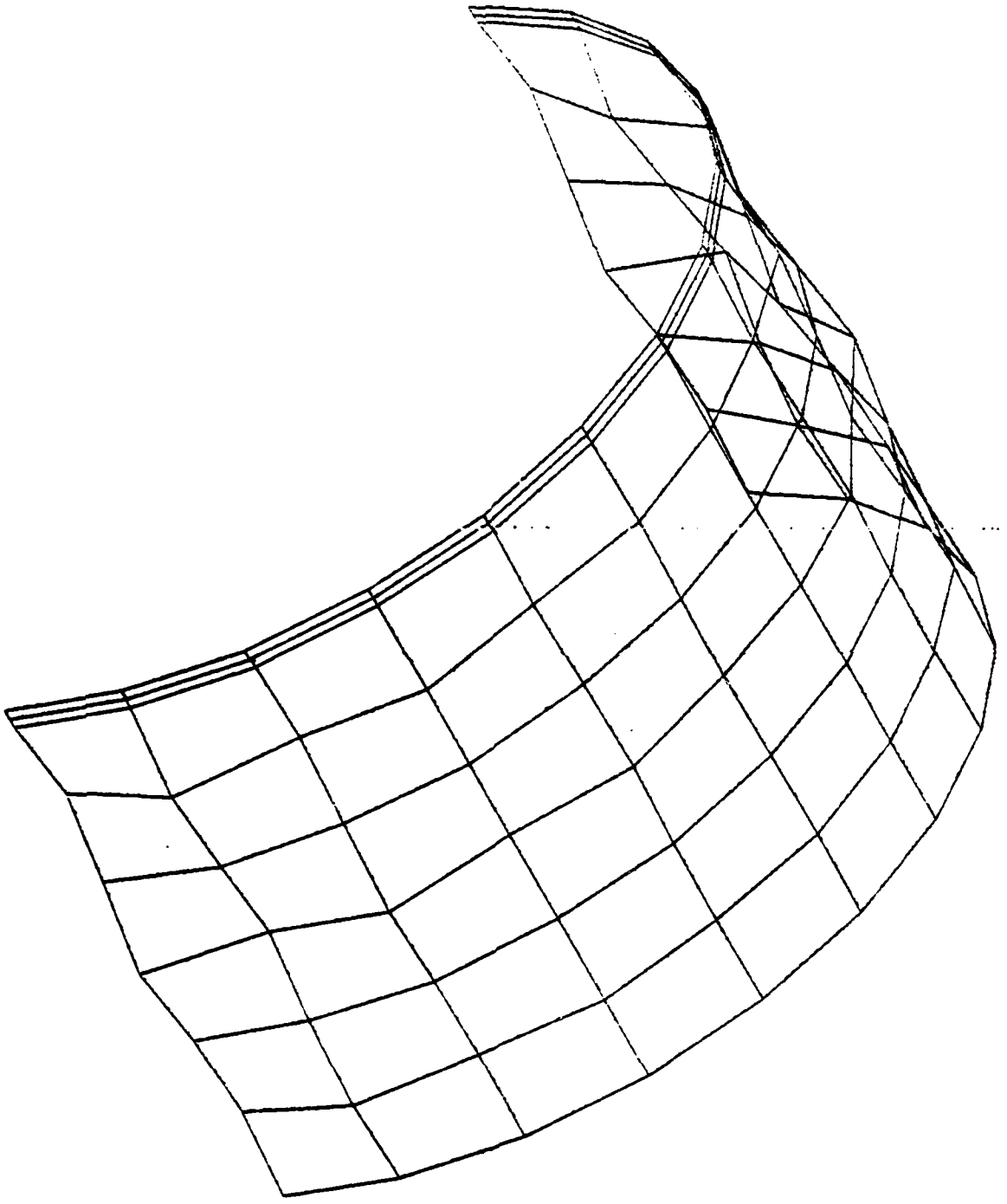

FIGURE 8. MODE 1 FOR MODEL 6 (ALUMINUM MODEL G OF MIDGLEY AND JOHNSON) SUBJECT TO CONTINUITY CONDITIONS AND W = 0 AT END 1

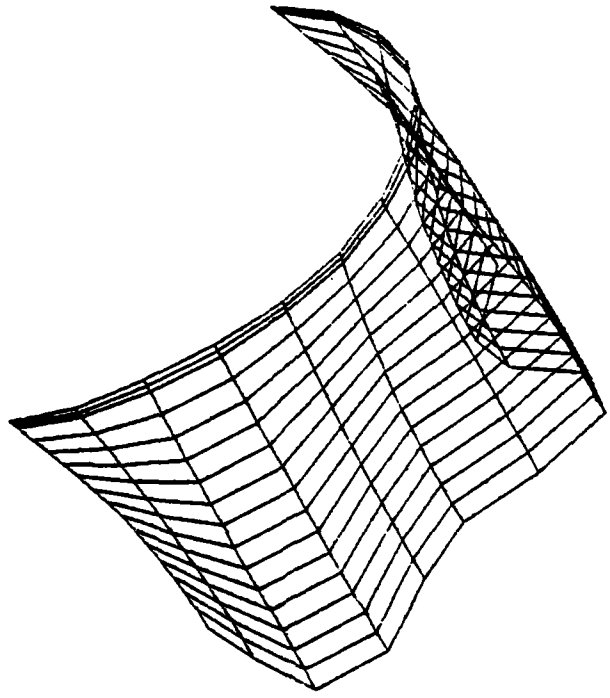

FIGURE 9. MODE 1 FOR MODEL 8 (ALUMINUM MODEL F OF MIDGLEY AND JOHNSON) SUBJECT TO SIMPLY SUPPORTED CONDITIONS AT END 1

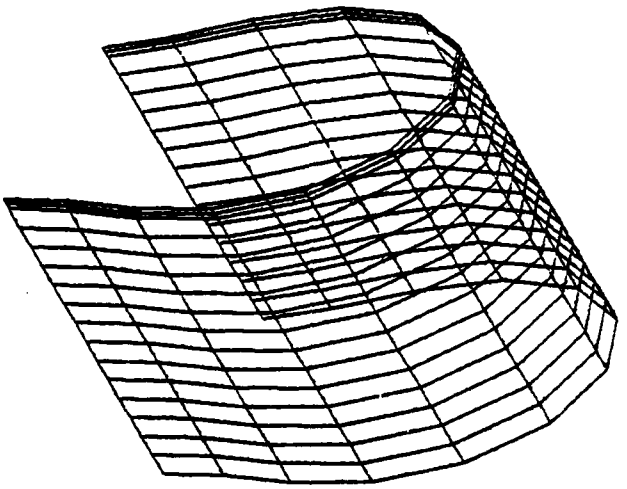

FIGURE 10. MODE 1 FOR MODEL 9 (ALUMINUM MODEL F OF MIDGLEY AND JOHNSON) SUBJECT TO CONTINUITY CONDITIONS AND $W \neq 0$ WITHOUT END RING AT END 1

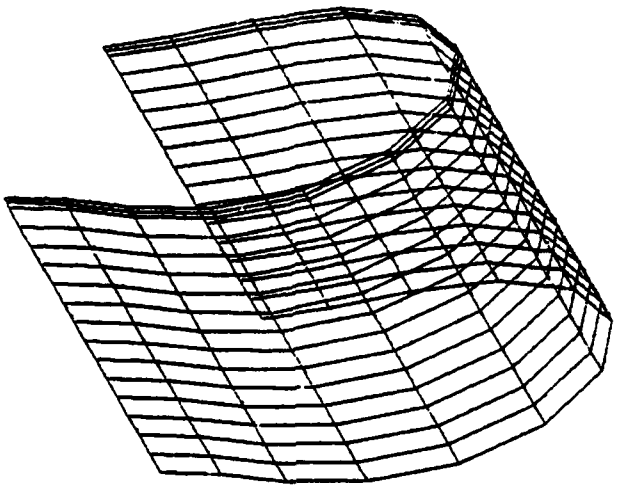

FIGURE 11. MODE 1 FOR MODEL 10 (ALUMINUM MODEL F OF MIDGLEY AND JOHNSON) SUBJECT TO CONTINUITY CONDITIONS AND W ≠ 0 WITH END RING AT END 1

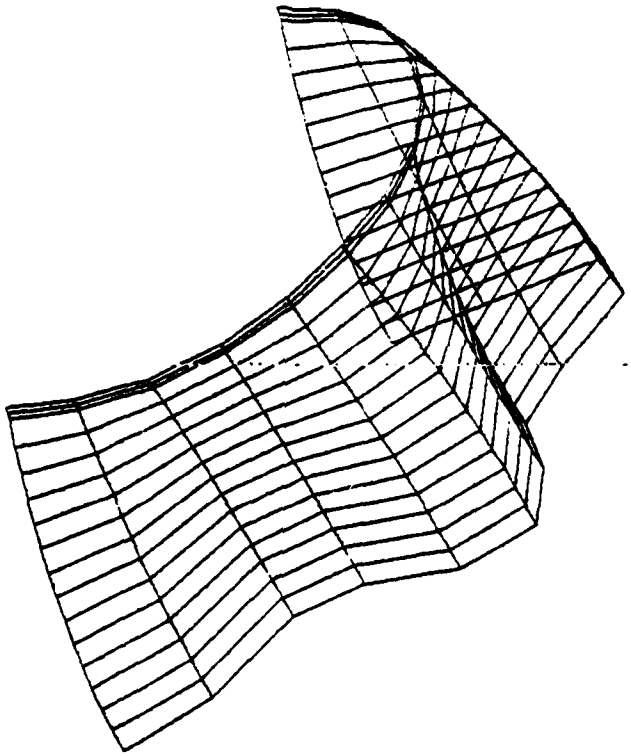

FIGURE 12. MODE 1 FOR MODEL 11 (ALUMINUM MODEL F OF MIDGLEY AND JOHNSON) SUBJECT TO CONTINUITY CONDITIONS AND W = 0 AT END 1

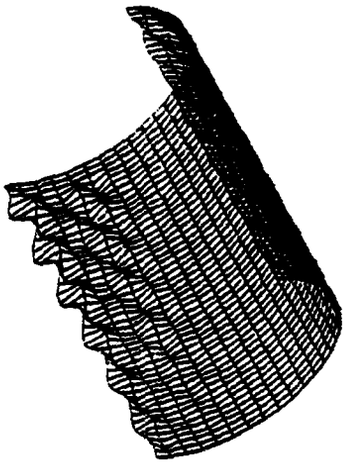

FIGURE 13. MODE 1 FOR MODEL 12 (STEEL 1/5 MODEL OF KINRA) SUBJECT TO CONTINUITY CONDITIONS AND W = 0 AT END 1

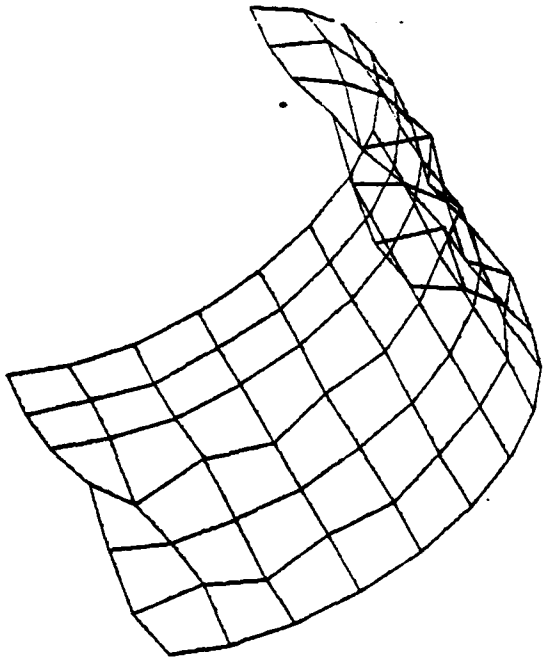

FIGURE 14. MODE 1 FOR MODEL 13 (BR-4, EXTERNALLY STIFFENED STEEL MODEL) SUBJECT TO CONTINUITY CONDITIONS AND W = 0 AT END 1

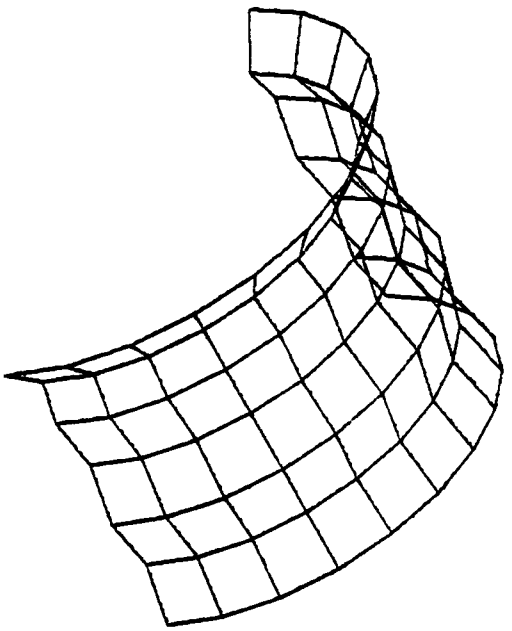

FIGURE 15. DEFORMED SHAPE OF MODEL 14 (STEEL MODEL BR-4) AT 500 Lb/in^2

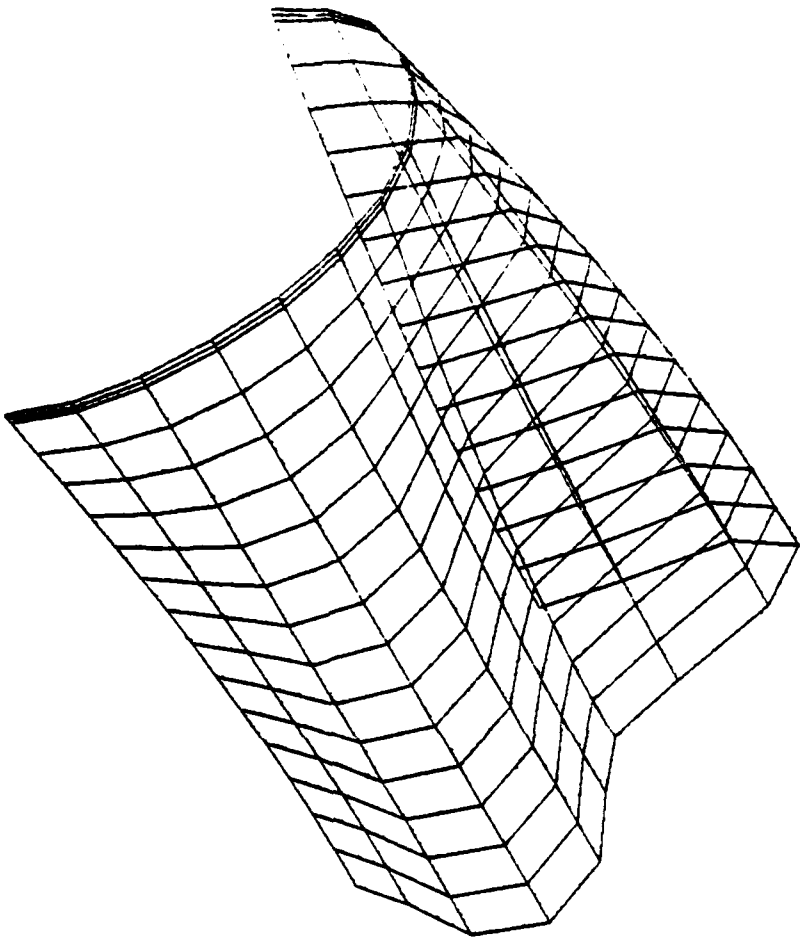

FIGURE 16. MODE 1 FOR MODEL 17 (1.965 LONGER THAN MODEL 8) SUBJECT TO SIMPLY SUPPORTED CONDITIONS AT END 1

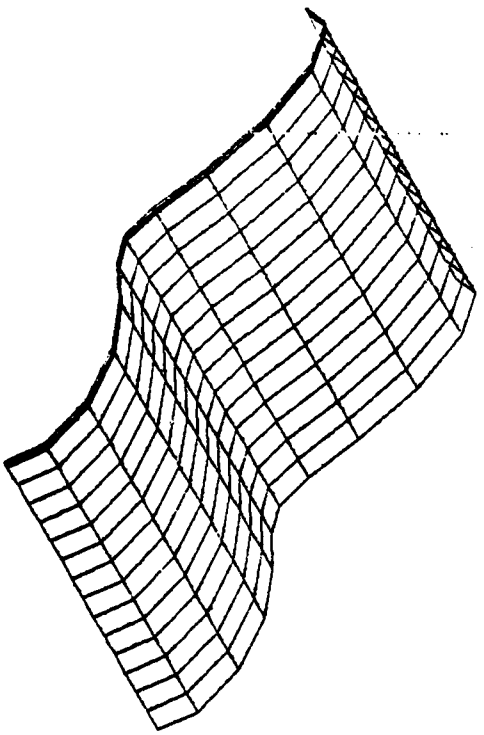

FIGURE 17. MODE 1 FOR MODEL 18 (1.965 LONGER THAN MODEL 9) SUBJECT TO CONTINUITY CONDITIONS AND $W \neq 0$, WITHOUT END RING AT END 1

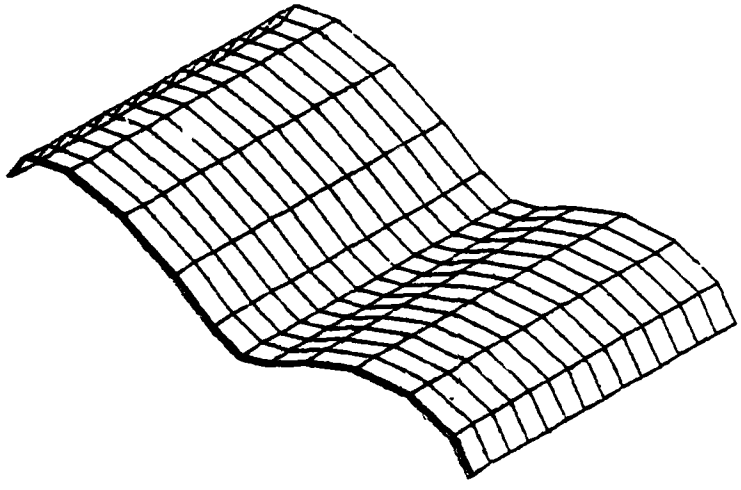

FIGURE 18. MODE 1 FOR MODEL 19 (1.965 LONGER THAN MODEL 10) SUBJECT TO CONTINUITY CONDITIONS AND $W \neq 0$, WITH END RING AT END 1

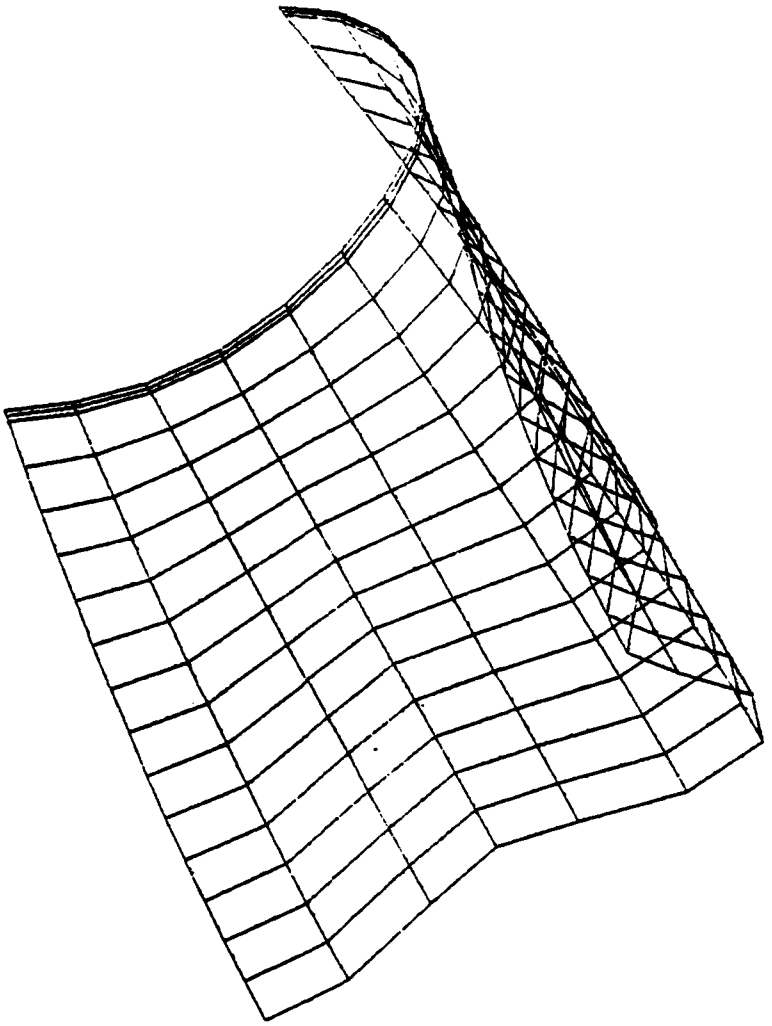

FIGURE 19. MODE 1 FOR MODEL 20(1.965 LONGER THAN MODEL 11) SUBJECT TO CONTINUITY CONDITIONS AND W = 0 AT END 1

TABLE 1. TEST MODEL STRUCTURAL DETAILS

MODEL NO.	1,1A,2	3	4-7	8-11	12	13,14	15,16	17-20
REF. NO.	3	7	8	8	9	4	6	8
TYPE OF STIFFENING	External	Internal	Internal	Internal	Internal	External	External	Internal
NO. OF BAYS	6 Excluding 2 At Ends	3 Equal	6 Equal Excluding 2 Ends	14 Equal Excluding 2 Ends	24 Equal Excluding 2 Uneven Ones	6 Unequal Excluding 2 At Ends	10 Unequal Excluding 2 Ends	14 Equal Excluding 2 Ends
RADIUS (IN)	13.375	5.000	7.970	7.970	28.675	14.410	13.4495	7.970
SKIN THICKNESS (IN)	0.062	0.550	0.030	0.040	0.113	0.1324	0.211	0.040
RADIUS TO THICKNESS RATIO	215.7	9.09	265.6	199.2	253.7	108.8	63.7	199.2
FRAME SPACING (IN)	5.27	7.50	3.10	1.30	6.00	7.11	2.57	2.60

TABLE 1. (Cont.)

WEB DEPTH (IN)	0.656	1.375	0.295	0.135	1.790	0.915	1.225	0.135
WEB THICKNESS (IN)	0.1875	0.350	0.105	0.105	0.116	0.231	0.330	0.105
LENGTH (IN)	30.984	22.500	19.250	18.850	149.75	44.360	27.22	37.05
LENGTH TO RADIUS RATIO	2.316	4.500	2.415	2.365	5.222	3.078	2.024	4.649

TABLE 2. TEST MODEL MATERIAL DETAILS

MODEL NO./ FEATURE	1,1A,2	3	4-7	8-11	12	13,14	15,16	17-20
MATERIAL	STEEL	AL (7075-T6)	AL (6061-T6)	AL (6061-T6)	STEEL (A36)	STEEL	STEEL (HTS)	AL (6061-T6)
ELASTIC MODULUS (psi)	30,000	10,400	10,100	10,100	30,000	30,000	30,000	10,100
PASSON'S RATIO	0.300	0.330	0.300	0.300	0.300	0.300	0.300	0.300
YIELD STRESS (psi)	54.40	72.50	35.00	35.00	32.60	50.60	59.60	35.00

TABLE 3. ACTUAL DIMENSIONS USED IN COMPUTATIONS

MODEL NO./ FEATURE	1,1A,2	3	4-7	8-11	12	13,14	15,16	17-20
NO. OF BAYS	2** Equidistant	1.5 Equidistant	3 Equidistant 1 Unequal	7 Equidistant 1 Unequal	12 Equidistant 1 Unequal	2 Equidistant 1 Unequal	4 Equidistant 1 Unequal	7 Equidstant 1 Unequal
MEAN RADIUS (IN)	13.3595*	4.725	7.9550	7.9550	28.6185	14.410	13.4495	7.9550
TOTAL LENGTH (IN)	10.540	11.250	9.625	9.425	74.875	19.220	12.340	18.525

* 13.344" is the actual mean radius
**Model 1A has 2 equal and 1 unequal bays

TABLE 4. MODELING DETAILS

FEATURE/ MODEL NO.	TOTAL DEGREES OF FREEDOM	NO. OF NODE RINGS BETWEEN FRAMES	DEGREE OF SYMMETRY	BOUNDARY CONDITION AT END 1*	BOUNDARY CONDITION AT END 2*
1	1350	3	Half Axially Half Circum-ferentially	RV=RW=0 W≠0 U≠0	RV=RW=0 U=0
1A	1950	3	Half Axially Half Circum-ferentially	RV=RW=0 W=0 U≠0	RV=RW=0 U=0
2	2646	3	Half Axially Full Circum-ferentially	RV=RW=0 W≠0 U≠0	RV=RW=0 U=0
3	1014	7&3	Half Axially Half Circum-ferentially	RV=RW=0 W≠0 U≠0	RV=RW=0 U=0
4	702	1	Half Axially Half Circum-ferentially	RV=RW=0 W=0 U≠0	RV=RW=0 U=0
5	702	1	Half Axially Half Circum-ferentially	RV=RW=0 W=0 U≠0	RV=RW=0 U=0
6	702	1	Half Axially Half Circum-ferentially	RV=RW=0 W=0 U≠0	RV=RW=0 U=0
7	702	1	Half Axially Half Circum-ferentially	RV=RW=0 W≠0 U≠0	RV=RW=0 U=0

*At both ends tangential displacement V=0 at 90° (and 270° for full model). For full Model No. 2 at θ=0 and θ=180° W=0. (In general W is free, if W≠0 is stated in boundary conditions).

TABLE 4. (Cont.)

FEATURE/ MODEL NO.	TOTAL DEGREES OF FREEDOM	NO. OF NODE RINGS BETWEEN FRAMES	DEGREE OF SYMMETRY	BOUNDARY CONDITION AT END 1*	BOUNDARY CONDITION AT END 2*
8	1326	1	Half Axially Half Circum-ferentially	V=W=RV=0 U≠0	RV=RW=0 U=0
9	1326	1	Half Axially Half Circum-ferentially	RV=RW=0 W≠0 U≠0	RV=RW=0 U=0
10	1326	1	Half Axially Half Circum-ferentially	RV=RW=0 W≠0 U≠0	RV=RW=0 U=0
11	1326	1	Half Axially Half Circum-ferentially	RV=RW=0 W=0 U≠0	RV=RW=0 U=0
12	7650	3	Half Axially Half Circum-ferentially	RV=RW=0 W=0 U≠0	RV=RW=0 U=0
13	546	1	Half Axially Half Circum-ferentially	RV=RW=0 W=0 U≠0	RV=RW=0 U=0
14	546	1	Half Axially Half Circum-ferentially	RV=RW=0 W=0 U≠0	RV=RW=0 U=0
15	858	1	Half Axially Half Circum-ferentially	RV=RW=0 W=0 U≠0	RV=RW=0 U=0

TABLE 4. (Cont.)

FEATURE/ MODEL NO.	TOTAL DEGREES OF FREEDOM	NO. OF NODE RINGS BETWEEN FRAMES	DEGREE OF SYMMETRY	BOUNDARY CONDITION AT END 1*	BOUNDARY CONDITION AT END 2*
16	858	1	Half Axially Half Circum-ferentially	RV=RW=0 W=0 U≠0	RV=RW=0 U=0
17	1326	1	Half Axially Half Circum-ferentially	V=W=RU=0 U≠0	RV=RW=0 U=0
18	1326	1	Half Axially Half Circum-ferentially	RV=RW=0 W≠0 U≠0	RV=RW=0 U=0
19	1326	1	Half Axially Half Circum-ferentially	RV=RW=0 W≠0 U≠0	RV=RW=0 U=0
20	1326	1	Half Axially Half Circum-ferentially	RV=RW=0 W=0 U≠0	RV=RW=0 U=0

TABLE 5. COMPARISON BETWEEN FINITE ELEMENT ANALYSIS PREDICTIONS AND EXPERIMENTAL RESULTS

DATA/ MODEL NO.	COLLAPSE PRESSURE PREDICTED BY STAGS (PSI)	EXPERIMENTAL COLLAPSE PRESSURE (PSI)	COLLAPSE MODE PREDICTED BY STAGS	EXPERIMENTAL COLLAPSE MODE	COLLAPSE PRESSURE (PSI) PREDICTED BY RING FORMULA, SOUTHWELL, VON MILES*
1	106.3	80	Oval	4 Lobes	114.8 96.5 114.9
1A	155.596	80	Local Buckling	4 Lobes	114.8 96.5 114.9
2	102.6	80	Oval	4 Lobes	114.8 96.5 114.9
3	9,500-10,500	9750	Plastic	Out of Round Model Failed Through Stiffener Collapse Than Plastic At Midbay	32,147.2 26,621.8 32,784.4
4	23.704	25.0	Local Buckling	Local Buckling Between Rings	16.4 19.5 23.1

*These approximate formulae employ elastic values. To incorporate plasticity effects we need to use tangent modulus etc.

TABLE 5. (Cont.)

DATA/ MODEL NO.	COLLAPSE PRESSURE PREDICTED BY STAGS (PSI)	EXPERIMENTAL COLLAPSE PRESSURE (PSI)	COLLAPSE MODE PREDICTED BY STAGS	EXPERIMENTAL COLLAPSE MODE	COLLAPSE PRESSURE (PSI) PREDICTED BY RING FORMULA, SOUTHWELL, VON MILES*
5	21.262	25.0	Oval	Local Buckling Between Rings	16.4 19.5 23.1
6	23.669	25.0	Local Buckling	Local Buckling Between Rings	16.4 19.5 23.1
7	Up To 32.0 No Collapse	25.0		Local Buckling Between Rings	16.4 19.5 23.1
8	62.651	65,68	General Instability	General Instability	
9	7.257	65,68	Oval	General Instability	5.2 95.8 138.7
10	7.524	65,68	Oval	General Instability	5.2 95.8 138.7

TABLE 5. (Cont.)

DATA/ MODEL NO.	COLLAPSE PRESSURE PREDICTED BY STAGS (PSI)	EXPERIMENTAL COLLAPSE PRESSURE (PSI)	COLLAPSE MODE PREDICTED BY STAGS	EXPERIMENTAL COLLAPSE MODE	COLLAPSE PRESSURE (PSI) PREDICTED BY RING FORMULA, SOUTHWELL, VON MILES*
11	62.371	65,68	General Instability	General Instability	5.2 95.8 138.7
12	161.19	110-115	Local Buckling	Buckling Between Rings	128.0 121.2 158.5
13	536.058	390	Local Buckling	2 Lobes	268.4 425.6 514.9
14	Up To 5125 No Collapse	390		2 Lobes	268.4 425.6 514.9
15	5540.3	1502		Axisymmetric	2475.2 4187.5 7222.2
16	Up To 1500 No Collapse	1502		Axisymmetric	3.03 47.9 58.9

TABLE 5. (CONT.)

DATA/ MODEL NO.	COLLAPSE PRESSURE PREDICTED BY STAGS (PSI)	EXPERIMENTAL COLLAPSE PRESSURE (PSI)	COLLAPSE MODE PREDICTED BY STAGS	EXPERIMENTAL COLLAPSE MODE	COLLAPSE PRESSURE (PSI) PREDICTED BY RING FORMULA, SOUTHWELL, VON MILES*
17	19.893		General Instability		3.03 47.9 58.9
18	4.13		Oval		3.03 47.9 58.9
19	4.268		Oval		3.03 47.9 58.9
20	20.277		General Instability		3.03 47.9 58.9

BIBLIOGRAPHY

Almroth, B. O., Brogan, F. A., and Stanley, G. M., Structural Analysis of General Shells, Vol. II. User Instruction for STAGSC, LMSC-D633873, Apr 1979.

Batista, R. C., and Croll, J. G. A., "Simple Buckling for Pressurized Cylinders," Journal of Engineering Mechanics EM5, ASCE, Oct 1982, pp. 927-944.

Blumenberg, W. F., and Reynolds, T. E., Elastic General Instability of Ring-Stiffened Cylinders with Intermediate Heavy Frames Under External Hydrostatic Pressure, DTMB Report 1588, Dec 1961.

Blumenberg, W. F., Hydrostatic Pressure Tests to Determine the Effect of Varying Degrees of End Fixity on the Elastic General Instability Strength of Ring-Stiffened Cylindrical Shells, DTMB Report 2361, May 1967.

Brush, D. O., and Almroth, B. O., Buckling of Bars, Plates, and Shells, McGraw Hill, Inc., 1975, pp. 161-167.

Bushnell, D., "Effect of Cold Bending and Welding on Buckling of Ring-Stiffened Cylinders," Journal of Computers and Structures, Vol. 12, 1980, pp. 291-307.

Coppa, A. P., "Measurement of Initial Geometrical Imperfections of Cylindrical Shells," AIAA Journal, Vol. 4, No. 1., Jan 1966, pp. 172-175.

DeHart, R., and Basdekas, N. L., "Investigation of Yield Collapse of Stiffened Circular Cylindrical Shells with a Given Out-of-Roundness," in Collected Papers on Instability of Shell Structures-1962, NASA TN D-1510, 1962, pp. 245-253.

Galletly, G. D., Slankard, R. C., and Wenk, E., Jr., "General Instability of Ring-Stiffened Cylindrical Shells Subject to External Hydrostatic Pressure-A Comparison of Theory," Journal of Applied Mechanics, Vol. 25, No. 2, Jun 1958, pp. 259-266.

Kinra, R. K., "Hydrostatic and Axial Collapse Tests of Stiffened Cylinders," Paper 2685 in Offshore Technology Conference, 1976, pp. 765-788.

Kirstein, A. F., and Slankard, R. C., An Experimental Investigation of the Shell-Instability Strength of a Machined, Ring-Stiffened Cylindrical Shell Under Hydrostatic Pressure (Model BR-4A), DTMB Report 997, Apr 1956.

BIBLIOGRAPHY (Cont.)

Krenzke, M. A., Effect of Initial Deflections and Residual Welding Stresses on Elastic Behavior and Collapse Pressure of Stiffened Cylinders Subjected to External Hydrostatic Pressure, DTMB Report 1327, Apr 1960.

Lunchick, M., and Overby, J. A., An Experimental Investigation of the Yield Strength of a Machined Ring-Stiffened Cylindrical Shell (Model BR-7M) Under Hydrostatic Pressure, DTMB Report 1255, Nov 1958.

Midgley, W. R., and Johnson, A. E., Jr., "Experimental Buckling of Internal Integral Ring-Stiffened Cylinders," Experimental Mechanics, Jul 1973, pp. 145-153.

Moussouros, M., Comparisons of Static Collapse Pressure Predictions of a Ring-Stiffened Cylindrical Shell Subject to Hydrostatic Pressure, NSWC TR 81-325, 3 Mar 1982.

Moussouros, M., Further Results on the Predictions of Collapse Pressure of a Ring-Stiffened Cylindrical Shell Subject to Hydrostatic Pressure, NSWC TR 82-172, Sep 1982.

Reynolds, T. E., and Blumenberg, W. F., General Instability of Ring-Stiffened Shells Subject to External Hydrostatic Pressure, DTMB Report 1324, Jun 1959.

Slankard, R. D., and Nash, W. A., Tests of the Elastic Stability of a Ring-Stiffened Cylindrical Shell, Model BR-5 (λ=1.705), Subjected to Hydrostatic Pressure, DTMB Report 822, May 1953.

Slankard, R. C., Tests of the Elastic Stability of a Ring-Stiffened Cylindrical Shell, Model BR-4 (λ=1.103) Subjected to Hydrostatic Pressure, DTMB Report 876, Feb 1955.

DISTRIBUTION

	Copies
Chief of Naval Material	
Attn: CAPT G. Jarrett (ASW-14)	1
Dr. A. J. Faulstich (MAT 07)	1
Navy Department	
Washington, DC 20360	
Commander	
Naval Sea Systems Command	
Attn: SEA-03B	1
SEA 05B (P. Palermo)	1
SEA 63R (F. Romano)	1
SEA-63R32 (Murphy)	1
SEA-9G32	1
SEA-32R (C. Pohler)	1
SEA-3221 (H. Ward)	1
PMS-402	1
PMS-406	1
PMS-407	1
Department of the Navy	
Washington, DC 20362	
Commander	
David W. Taylor Naval Ship Research & Development Center	
Attn: Code 17 (Dr. W. Murray)	1
Code 175 (J. Sykes)	1
Code 175.2 (B. Whang)	1
Code 175.2 (T. Giacofci)	1
Code 175.2 (T. Gilbert)	1
Code 175.3 (W. Conley)	1
Code 175.3 (P. Manny)	1
Code 184.4 (M. Hurwitz)	1
Code 172 (M. Krenzke)	1
Code 1720.3 (R. Jones)	1
Bethesda, MD 20084	

	Copies
David W. Taylor Naval Ship Research & Development Center	
Attn: Code 177 (R. Fuss)	1
Code 177.1 (V. Bloodgood)	1
Code 177.1 (M. Riley)	1
Code 177.1 (R. Higginbotham)	1
Underwater Explosion Research Division	
Portsmouth, VA 23709	
Naval Coastal Systems Center	
Attn: Code 4210 (J. Rumbough)	1
Panama City, FL 32407	
Lockheed Palo Alto Laboratory	
Lockheed Missiles and Space Company Labs	
Attn: Thomas L. Geers	1
3251 Hanover Street	
Palo Alto, CA 94304	
Commander	
Naval Weapons Center	
Attn: Code 533 (Technical Library)	1
China Lake, CA 93555	
Commander	
Naval Ocean Systems Center	
Attn: Technical Library	1
San Diego, CA 92152	
Commanding Officer	
Naval Underwater Systems Center	
Attn: (D. J. Lepore)	1
Newport, RI 02840	

DISTRIBUTION (Cont.)

	Copies
Office of Naval Research Attn: Code 474 (D. N. Basdekas) 800 North Quincy Street Arlington, VA 22217	1
Defense Nuclear Agency Attn: SPSS (LT D. Sobota) Washington, DC 20305	1
Defense Technical Information Center Cameron Station Alexandria, VA 22314	12
Library of Congress Attn: Gift and Exchange Division Washington, DC 20540	4
Internal Distribution:	
R10	1
R102	2
R14	20
R14 (M. Moussouros)	1
E431	9
E432	3
E35	1

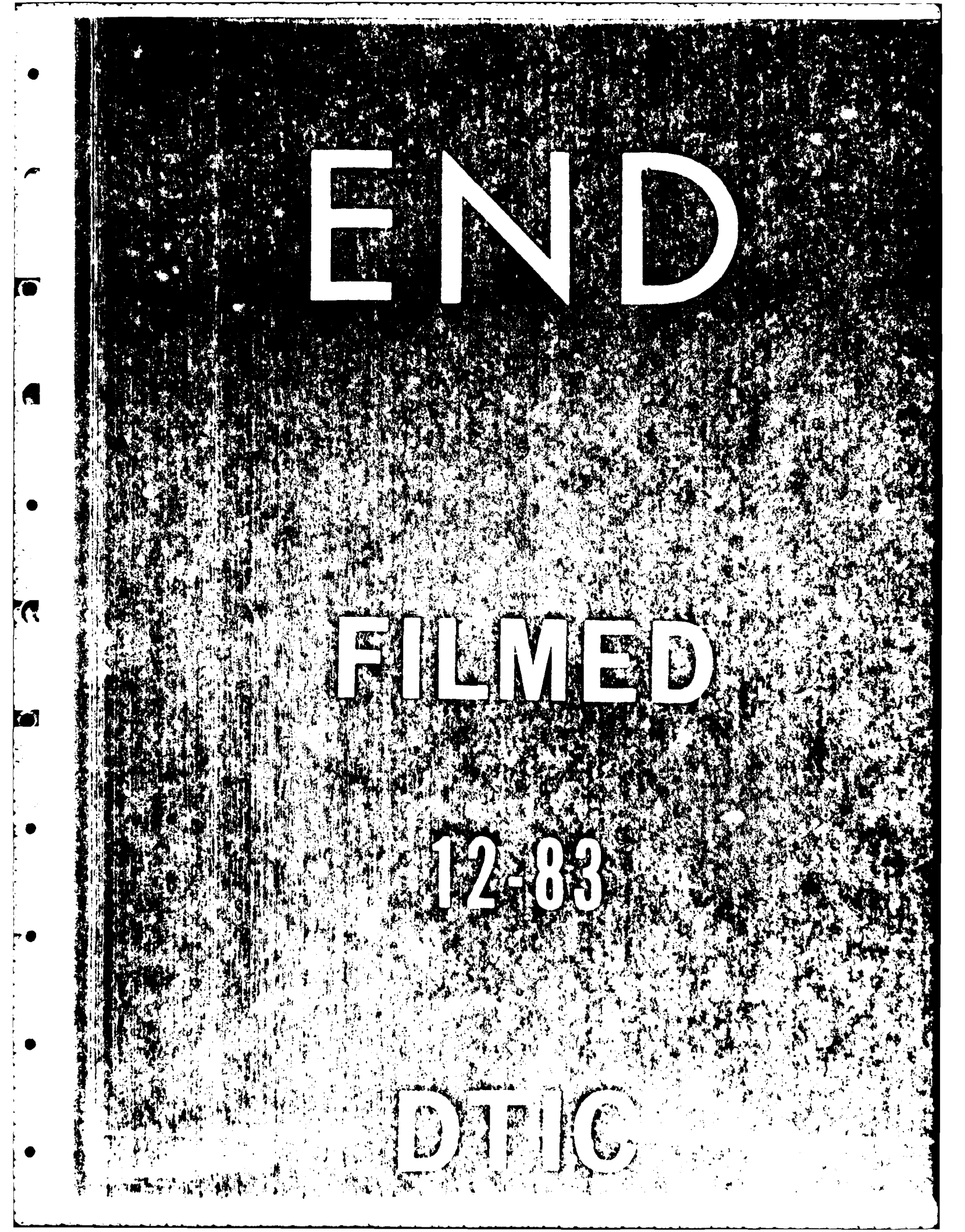
END
FILMED
12-83
DTIC